

Novel Methodology to Assess RF Performance of Co-located MIMO Radar Systems Transmitting Binary Phased Coded Waveforms

Nivia Colon-Diaz^{1,2}, Dan Janning¹, Patrick M. McCormick¹, James T. Aberle²,
and Daniel W. Bliss²

¹ Sensors Directorate, Air Force Research Laboratory, Wright-Patterson Air Force Base, OH
nivia.colon_diaz.3@us.af.mil

² Department of Electrical, Computer, and Energy Engineering, Arizona State University, Tempe, AZ

Abstract — In this work an experimental radar testbed and dual directional couplers (DDC) are used to collect measurements of the forward and reverse waves at each element, its mutual coupling, and beam-patterns. The collected measured data is used to validate a methodology for assessing radio frequency (RF) performance of a co-located multiple-input multiple-output (MIMO) radar system transmitting binary phased coded (BP) waveforms. The estimated and measured active reflection coefficient (ARC) and beam-patterns are presented. The effect of different excitations and mutual coupling on the radiated fields is also presented.

Index Terms — Active reflection coefficient, co-located MIMO radar, coupled power, mutual coupling.

I. INTRODUCTION

Radio Frequency (RF) sensors are maturing into fully digital systems characterized by a wide-band frequency range and capable of performing multiple tasks simultaneously on different elements or sub-arrays. These RF sensors are also evolving towards a capability to execute simultaneous functions such as electronic warfare, communications, and radar tasks such as search, detect, track and image a target. Early digital signal processing research on these type of sensors [1] ignored electromagnetic effects, such as interactions between elements or mutual coupling.

As commercial communication and defense systems are consuming more spectrum [2], multi-functional operation demands techniques to alleviate spectral congestion and improve the efficiency by sharing the spectrum. Multiple-input multiple-output (MIMO) emissions enable multi-functionality via simultaneous transmission of independently modulated waveforms in the same band from different radiators or sub-arrays. While MIMO techniques could be the key approach to accommodate multi-function operations, the concept demands careful understanding of how each function,

subsystem, and/or sub-array, interacts with one another while ensuring enough isolation among them [3]. Previous work developed by the authors [4-5] presents a way to assess mutual coupling effects by analyzing the active reflection coefficient (ARC) and active voltage standing wave ratio (VSWR) and quantifying their impact on beam-patterns.

The benefits of improving our understanding of mutual coupling effects on MIMO radar systems are two-fold. First, the knowledge can enhance MIMO radar calibration techniques and provide key information to system designers [6]. Second, MIMO radar waveform design can take advantage of new discoveries to use the waveforms designed specifically for transmit mode and improve signal-to-noise ratio performance [7], beam-pattern and side-lobe levels [8] and other metrics.

In this paper, we present beam-pattern and ARC measurements obtained using U.S. Air Force Research Laboratory (AFRL) Baseband-digital at Every Element MIMO Experimental Radar (BEEMER) for a uniform linear array (ULA) of 6 patch antennas linearly placed with a separation of 0.5λ and transmitting binary phased coded (BP) waveforms. Even though the methodology can be applied to any transmit waveform, this initial study uses BP waveforms. The objectives of this paper are to (1) validate the methodology developed previously by directly measuring the ARC and the beam-patterns on co-located MIMO radars and (2) analyze the effects that mutual coupling and excitations have in the radiated fields on a MIMO radar transmission.

II. MUTUAL COUPLING ANALYSIS

Ideally, a signal radiated by the m -th element of a ULA would only radiate from the phase center of the m -th element without affecting adjacent elements. In reality, real antenna arrays experience mutual coupling in which the signal radiated by the m -th element will couple into neighboring elements. This has two consequences: the signal transmitted by the m -th element

1) can be observed by a receiver connected to the n -th element and 2) can be re-radiated from the phase center of the n -th element at a reduced power and coupling which will alter the array's beam-pattern.

Direct measurements of the ARC were collected using dual directional couplers (DDCs) (Hewlett Packard 777D 1.9-4GHz with -20 dB coupling factor), as described in [5]. A DDC can be equivalently modeled as two directional couplers with their isolated ports terminated as described in [9]. The majority of the signal fed to the input port will be transmitted to the output port with a portion of the signal coupled to the forward port. A signal entering through the output port will couple into the reverse port. The calibrated ratio between the reverse and forward waves can be used to compute the ARC via:

$$\Gamma_n^a = \frac{b_n}{a_n} = \frac{\sum S_{nm} a_m}{a_n}, \quad (1)$$

where Γ_n^a is the ARC observed in antenna n due to the other m elements, a_n represents the amplitude and phase of the forward wave on element n (defined as the excitation of antenna n), and b_n represents the amplitude and phase of the reverse wave in antenna n . S_{nm} is the conventional scattering (S) parameter defined as the passive ratio of the signal coupled to port n from a signal incident on port m , when all other ports are terminated in the system impedance [10]. A block diagram showing the main components required to perform this measurement is given in Fig. 1. The DDCs were connected directly to the 6 antenna patch elements of the ULA, the other 4 antenna elements were matched terminated, as shown in Fig. 1. A description of the single multilayer patch antenna can be found in [11]. The coupled ports of each DDC were then used to measure the signals sent to and reversed from each radiator. To collect ARC measurements, BEEMER was configured to provide 6 transmit and 12 receive channels (6 forward coupled and 6 reversed coupled) so that all measurements could be collected simultaneously.

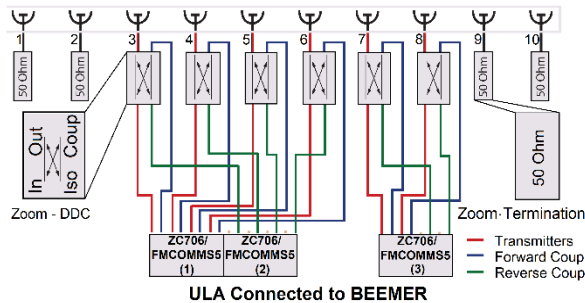


Fig. 1. BEEMER and DDC connections to directly collect ARC measurements using the FPGA ZC706 board and the 4-channel FMCOMMS5 transceiver.

The S-matrix of a 6x1 linear sub-array of horizontally polarized radiators formed from a 10x6 dual polarized

patch array was measured with the unused elements terminated. An Agilent Technologies M9375A vector network analyzer with 16 channels was used to measure the S-parameters at 3.5 GHz. The measured S-parameters and Equation (1) were used to obtain the estimated ARC [12]. The estimated ARC is compared to the directly measured ARC using the DDCs following the method developed in [5] are presented in Table 1. Good agreement between estimates and measurements of the ARC can be seen in Table 1.

The BEEMER system is constructed from commercial off the shelf components [13]. The principal components are a ZC706 field-programmable gate array (FPGA) board and an FMCOMMS5 4-channel transceiver. The system has the ability to synchronize multiple ZC706's/FMCOMMS5's to provide ≥ 4 transceiver channels. Arbitrary waveforms can be sent on each channel, which allows MIMO transmission to be studied. BEEMER's maximum sampling rate is 60 Mega samples per second, its maximum transmitted signal length is 4096 samples, the center frequency selected is 3.5 GHz and the transmitted power is -8 dBm.

Table 1: Estimated and measured ARC on each channel

Channel	Estimated [dB]	Measured [dB]
1	-17.8	-17.8
2	-15.9	-15.0
3	-17.2	-19.4
4	-15.0	-16.5
5	-15.6	-16.6
6	-16.8	-18.8

To obtain beam-pattern data, BEEMER was triggered to transmit on 6 channels using BP waveforms and to record the signal observed. The waveforms were 1024 samples long. For each azimuth angle (-90 to 90), BEEMER transmitted simultaneously on each channel and the waveform on each channel was repeated 256 times at each angle. BEEMER received 2000 x 16 x 256 matrix of data at each azimuth location (where the dimensions are fast time x channel x slow time). Measurements were collected in the anechoic chamber seen in Fig. 2.

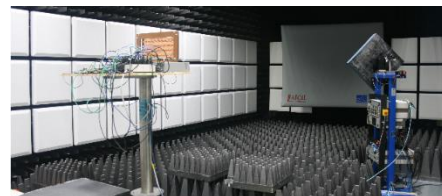


Fig. 2. BEEMER configuration in anechoic chamber.

In typical radar applications, the data collected is saved in a data cube with three dimensions: fast time (range), slow time (pulse to pulse), and channels.

Channels 1-6 collected reverse coupling, channels 7-12 recorded forward coupling, channel 13 was connected to the feed antenna (via a long SMA coaxial cable and an amplifier was placed just behind the feed antenna to compensate cables losses while minimizing the noise figure), and channels 14-16 were match terminated. The matrix was summed along the slow time dimension to coherently integrate the data while pulse compression was applied to the fast time dimension (to reduce the 2000 samples to a single sample per azimuth angle).

III. ANALYSIS ON RADIATED FIELDS

A MIMO transmission has a time-varying amplitude/phase array excitation from the superposition of independently generated waveform modulations. A MIMO radar illuminates the entire surveillance volume with each pulse, rather than sweeping a beam through the search area as a traditional phased array might. For this analysis, the fields of a MIMO transmission are characterized for a single time instant. Because each element radiates a different waveform, mutual coupling must be considered.

An approximation to the total radiated fields of a MIMO transmission, considering mutual coupling and different excitations can be represented in Equation (2) [14]. A special case of this equation is when mutual coupling is ignored ($\Gamma_n^a = 0$). This special case is known as the pattern multiplication concept and presents the approximation to the radiated fields used by early researchers. The pattern multiplication concept assumes that the element current distribution does not vary from element to element:

$$E(\theta, \phi) \approx f^i(\theta, \phi) \sum_{n=1}^N (1 - \Gamma_n^a) a_n e^{jk(n-1)(x_n u + y_n v)}, \quad (2)$$

where $f^i(\theta, \phi)$ is the isolated element pattern, N is the number of elements in the array, with $u = \sin \theta \cos \phi$ and $v = \sin \theta \sin \phi$, coupling effects are captured with Γ_n^a (the ARC), the different excitations are considered with a_n , the $e^{jk(x_n u + y_n v)}$ accounts for element positions, geometrical configuration, and inter-element spacing between elements, with (x_n, y_n) the coordinates of each element on the xy -plane. The radiated fields of an isolated antenna element pattern were modeled using a finite element-boundary integral computational electromagnetic tool SENTRI, as shown in Fig. 3.

Figures 4-5 present predicted beam-patterns in the (u, v) space in normalized dB, using Equation (2) with the isolated patch antenna pattern $f^i(\theta, \phi)$ from SENTRI, as seen in Fig. 3. In Fig. 4 the fields are generated with $\Gamma_n^a = 0$ and unitary excitations ($a_n = 1$), showing that the far zone field follows the multiplication of the isolated element pattern with the array factor neglecting coupling. Figure 5 displays the fields with $a_n = [e^{j\pi}, e^{j\pi}, e^{j0}, e^{j0}, e^{j\pi}, e^{j\pi}]$ and $\Gamma_n^a \neq 0$, calculated using Equation (1). Comparing Figs. 4 and 5, one can observe the array directivity is affected by coupling

and the selected excitation. These parameters must be considered in the design of the system and its waveforms.

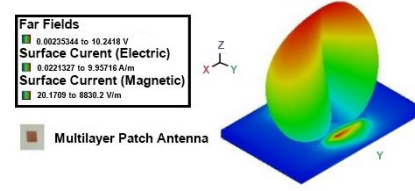


Fig. 3. Predicted fields of multilayer patch antenna.

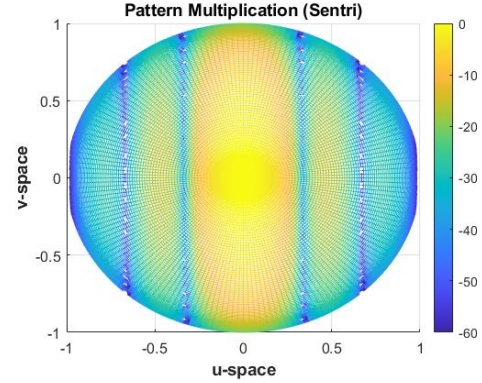


Fig. 4. Predicted radiated fields of a MIMO radar using pattern multiplication concept ($\Gamma_n^a = 0$).

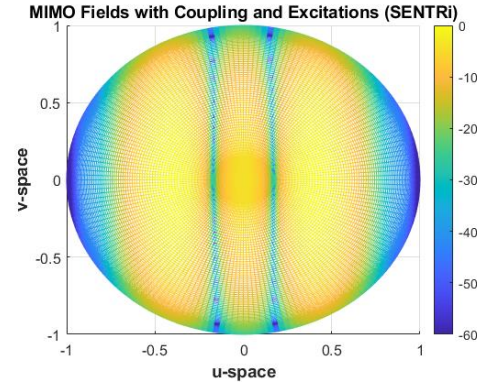


Fig. 5. Predicted fields of a MIMO radar considering coupling and binary phased excitations.

Figures 6-7 present predicted and measured fields at an instant in time. The blue-'x' and blue-solid curves depict the measured and predicted fields, respectively, when transmitting uniform excitations ($a_n = 1$). The predicted fields were obtained as previously described for Figs. 4-5 with $\Gamma_n^a \neq 0$. The measured fields were obtained using the BEEMER testbed through channel 13 as explained in Section II. The black curves on Fig. 6 present the predicted (black-dotted) and measured (black-squared) fields with excitations from Case 1 with $a_n = [e^{j0}, e^{j0}, e^{j\pi}, e^{j\pi}, e^{j\pi}, e^{j\pi}]$. The black curves

on Fig. 7 show predicted and measured fields with $a_n = [e^{j\pi}, e^{j\pi}, e^{j\pi}, e^{j\pi}, e^{j0}, e^{j0}, e^{j0}]$ from Case 2. Predicted and measured fields follow the same trend and validate the methodologies used in this work. One can observe in Figs. 6-7 that the side-lobe levels and the location of the nulls vary depending on the coupling and controlled through the excitation.

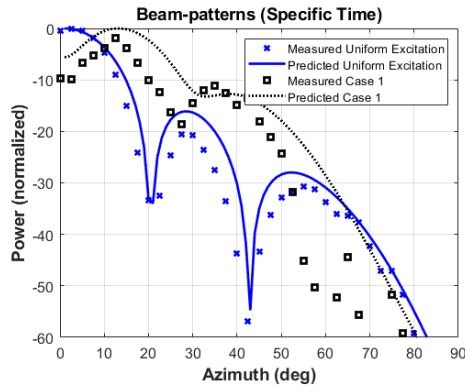


Fig. 6. Measured and predicted fields for a time instant, with uniform and Case 1 excitations.

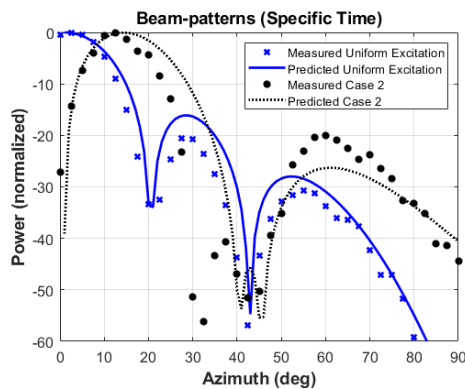


Fig. 7. Measured and predicted fields for a time instant, with uniform and Case 2 excitations.

IV. CONCLUSIONS

A methodology of co-located MIMO radars for estimating and directly measuring the ARC by using a DDC in each radiator is validated. These are the first direct measurements of reverse and forward coupled waves for co-located MIMO radars. Understanding reverse waves ensures the safety of the system and the prevention of large power reflections. This becomes important in high power applications where the reversed energy can be large enough to damage the transmitter. The impact of coupling and excitations on the beam-pattern, at an instant in time, can assist in identifying isolated effects. Figures 4-7 demonstrate that mutual coupling and the excitations of the elements play an important role in the performance of the radiation pattern

and the directivity of a co-located MIMO radar system. These parameters must be considered in the design of the system and its waveforms.

REFERENCES

- [1] H. V. Trees, *Optimum Array Processing (Detection, Estimation, and Modulation Theory, Part IV)*, 1st ed., Wiley-Interscience, New York, 2002.
- [2] A. R. Chiriyath, S. Ragi, H. D. Mittelmann, and D. W. Bliss, "Novel radar waveform optimization for a cooperative radar-communications system," *IEEE Trans. on Aerospace and Electr. Syst.*, pp. 1-1, 2019.
- [3] C. I. Coman, I. E. Lager, and L. P. Lighthart, "Multifunction antennas - the interleaved sparse sub-arrays approach," *2006 European Radar Conference*, Sept. 2006.
- [4] N. Colon-Diaz, J. G. Metcalf, D. Janning, and B. Himed, "Mutual coupling analysis for collocated MIMO radar applications using CEM modeling," *IEEE Radar Conf.*, May 2017.
- [5] N. Colon-Diaz, D. Janning, T. Corigliano, L. Wang, and J. Aberle, "Measurement of active reflection coefficient for co-located MIMO radar using dual directional couplers," *2018 AMTA Proc.*, Nov. 2018.
- [6] C. M. Schmid, C. Pfeffer, R. Feger, and A. Stelzer, "An FMCW MIMO radar calibration and mutual coupling compensation approach," *2013 European Radar Conference*, Oct. 2013.
- [7] B. T. Arnold and M. A. Jensen, "The effect of antenna mutual coupling on MIMO radar system performance," *IEEE Transactions on Antennas and Prop.*, vol. 67, no. 3, pp. 1410-1416, Mar. 2019.
- [8] P. M. McCormick, S. D. Blunt, and J. G. Metcalf, "Wideband MIMO frequency modulated emission design with space-frequency nulling," *IEEE J. Sel. Top Sig. Pro.*, vol. 11, no. 2, pp. 363-378, Mar. 2017.
- [9] J. Jorgesen and C. Marki, "Directivity and VSWR Measurements, Understanding Return Loss Measurements," *Marki Microwave*, 2012.
- [10] D. M. Pozar, *Microwave Engineering*. 4 ed., Wiley, Hoboken, 2011.
- [11] B. Baumen, A. Christianson, A. J. Wegener, and W. J. Chappell, "Dynamic visualization of antenna patterns and phased-array beamsteering," *IEEE Antennas and Propagation Magazine*, vol. 54, no. 3, pp. 184-198, 2012.
- [12] C. Zhang, Q. Lai, and C. Gao, "Measurement of active s-parameters on array antenna using directional couplers," *2017 IEEE Asia Pacific Microwave Conference (APMC)*, Nov. 2017.
- [13] T. C. Mealey and A. J. Duly, "BEEMER a firmware-tuned, software defined MIMO radar testbed," *2016 IEEE International Symposium on Phased Array Systems and Technology*, Oct. 2016.
- [14] L. Savy and M. Lesturgie, "Coupling effects in MIMO phased array," *2016 IEEE Radar Conf.*, 2016.